



ISSN: 0067-2904

## A Prediction of Skin Cancer using Mean-Shift Algorithm with Deep Forest Classifier

V. Gokula Krishnan<sup>1\*</sup>, K. Sreerama Murthy<sup>2</sup>, Srinivasarao Kongara<sup>3</sup>, Kurra Upendra Chowdary<sup>4</sup>, M. Somaskandan<sup>5</sup>, A. Jerrin Simla<sup>6</sup>

<sup>1</sup>Professor, CSE Department, Saveetha School of Engineering, SIMATS, Chennai, Tamil Nadu, India

<sup>2</sup>Associate Professor, IT Department, Sreenidhi Institute of Science and Technology, Hyderabad, TS, India

<sup>3</sup>Assistant Professor, CSBS Department, RVR & JC College of Engineering, Guntur, Andhra Pradesh, India

<sup>4</sup>Assistant Professor, CSBS Department, RVR & JC College of Engineering, Guntur, Andhra Pradesh, India

<sup>5</sup>Assistant Professor, IT Department, Panimalar Engineering College, Chennai, Tamil Nadu, India

<sup>6</sup>Associate Professor, CSE Department, Panimalar Institute of Technology, Chennai, Tamil Nadu, India

Received: 27/11/2021

Accepted: 18/2/2022

Published: 30/7/2022

### Abstract

Skin cancer is the most serious health problems in the globe because of its high occurrence compared to other types of cancer. Melanoma and non-melanoma are the two most common kinds of skin cancer. One of the most difficult problems in medical image processing is the automatic detection of skin cancer. Skin melanoma is classified as either benign or malignant based on the results of this test. Impediment due to artifacts in dermoscopic images impacts the analytic activity and decreases the precision level. In this research work, an automatic technique including segmentation and classification is proposed. Initially, pre-processing technique called DullRazor tool is used for hair removal process and semi-supervised mean-shift algorithm is used for segmenting the affected areas of skin cancer images. Finally, these segmented images are given to a deep learning classifier called Deep forest for prediction of skin cancer. The experiments are carried out on two publicly available datasets called ISIC-2019 and HAM10000 datasets for the analysis of segmentation and classification. From the outcomes, it is clearly verified that the projected model achieved better performance than the existing deep learning techniques.

**Keywords:** Benign; Deep Forest Classifier; Hair Removal; Malignant; Segmentation; Classification; Skin Cancer Detection.

### 1. Introduction

Cancer is the foremost cause of mortality in the world, agreeing to the World Health Organization (WHO). Over the next few decades, the number of people diagnosed with cancer is expected to double [1]. Skin cancer (SC) is one of the most prevalent lethal tumours among populations, with over 9% of them being diagnosed in the United States [2]. The sum of people diagnosed with SC has increased dramatically in recent decades in countries [3–5]. In addition, agreeing to the Brazilian Cancer Institute (INCA), 33% of cancer cases in Brazil are caused by SC. The death toll and infection rates from SC are still rising [6]. Cancer mortality rates can be reduced if it is discovered and treated early. The key to improve

\*Email: [gokul\\_kris143@yahoo.com](mailto:gokul_kris143@yahoo.com)

outcomes is early diagnosis of SC, which has been linked to a significant rise in the survival rate. Even if the disease progresses before the skin, there is a low survival chance [7].

The early procedures proposed in the literature were designed to improve the initial evaluation of melanoma images taken with a "dermoscope". The Glasgow 7-point checklist [8] is the most well-known of these algorithms, and it emphasises that changes in the size, shape, and colour of the pigmented lesion are the primary signals in selecting patients for referral. Abbasi et al. [9] proposed adding mole development to the ABCD (asymmetry, border indiscretion, colour change, and dimension) criteria, making it ABCDE (asymmetry, border anomaly, colour variation, and evolution of moles). Oliveira et al. [10] suggested a similar method for detecting and categorising skin lesions in macroscopic pictures using ABCD characteristics and texture analysis.

These algorithms are not intended to filter skin lesion photos obtained by a regular consumer-grade digital camera or a dermoscope in a dynamic and unrestrained environment. Underutilization of dermoscopy by dermatologists in practise has been observed [11], with the primary cause being a lack of training or interest. A physician can also do a skin cancer screening; however it can also be done on oneself using consumer-grade imaging technologies. Digital medical photos can be sent to an expert for consultation via the internet using the provided communication facility.

In this work, we present a scheme that is accomplished of professionally performing segmentation and classification of dermoscopic skin cancer images [12]. Hair removal process is carried out by using DullRazor tool, where segmentation of input images is done by using semi-supervised mean-shift algorithm. The experiments are conducted on the dermoscopic images from ISIC grand challenge 2019 and HAM10000 [13-14] dataset in terms of major parameter metrics. This research paper is constructed as follows: Section 2 presents study of various existing techniques that are developed to recognise the skin cancer. The explanation of proposed segmentation and classification model is given in Section 3. The experimental analysis of proposed model with existing techniques on two publicly available dataset is provided in Section 4. Finally, the scientific contribution of the study with future development is defined in Section 5.

## 2. Related Works

For example, Hameed et al. [15] presented an algorithm that uses Alexnet-pertained CNNs to identify and categorise skin illnesses such as benign and malignant using ECOC SVM. The accuracy of the results is low, i.e.86.21%. Ahmed, et al. [16] uses the ACO-GA method, which has a segmentation accuracy of 94%, in conjunction with a hybrid genetic algorithm. The GLCM and transductive SVM (TSVM) procedures are used to extract and classify feature information. The fitness function contributes 95 percent of the overall system accuracy. The system would be more efficient if any other method was used in conjunction with GLCM. K-means clustering is utilised to segment the lesion images, and LBP-based GLCM is used to extract features from the images in another research Khan et al. [17]. Classification is done using SVM.

Hameed, et al. [18] used the Otsu thresholding method, an automated system can identify the area of interest (ROI) of a skin lesion section. To extract features, the approach employs several colour models, GLCM, and NGTDM (neighbourhood gray-tone alteration matrix). Classification of skin illnesses such as acne, eczema, psoriasis, malignant melanoma and benign melanoma is done using the SVM (quadratic kernel). Only about 83% of the predictions are correct.

CNN models outperformed humans for the first time in 2019, according to a study by Brinker et al. [19], the 145 dermatologists trained ResNet50 on clinical MED-NODE database photos generated an accuracy of 89.4 percent for the ISIC archive images and 67.2 percent for the clinical images in the ISIC archive. Images taken via dermoscopy can improve the results of a

CNN. On the HAM10000 dataset, Mohamed et al., [20] developed a model based on MobileNet that achieved 92.7 percent accuracy. With HAM10000, Chaturvedi et al. have developed and organised a high-performance web application that utilises MobileNet model data and attains an accuracy rate of 83.1 percent in [21].

### 3. Proposed Work

In this section, skin cancer disease prediction process is carried out by two processes, such as segmentation and classification which is described in Figure 1. Initially, the input image is taken from ISIC challenging datasets of 2019 and HAM10000. To remove the hair from the input images, DullRazon tool is presented in the proposed research, where mean-shift algorithm is used for segmentation. Finally, the segmented image is converted into  $20 \times 20$  matrix and given as an input to the Deep Forest Classifier. These processes are briefly explained in the following below section.

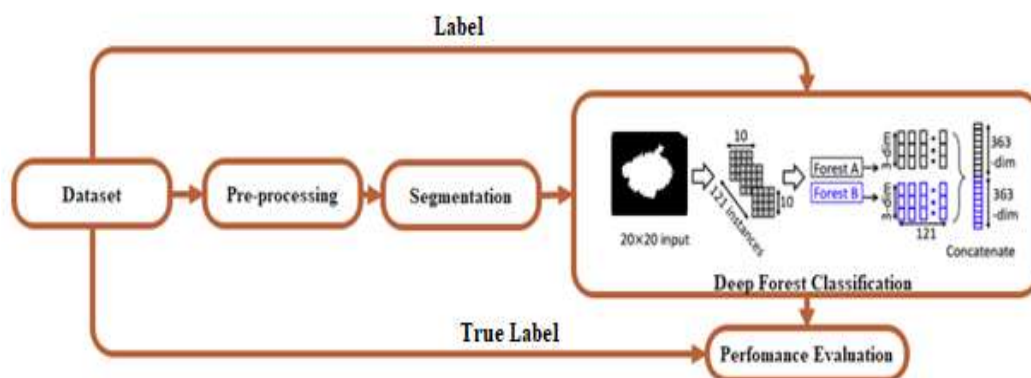


**Figure 1-**Working Flow of the Proposed System

#### 3.1. Dataset.

The proposed system evaluated with the help of two different datasets such as ISIC 2019 and HAM10000. The detail description of the data sets defined in the below section.

##### 3.1.1. ISIC 2019

The dataset is acquired from ISIC (International skin imaging collaboration) 2019 challenge dataset archive which contains benign and malignant lesions dermoscopy images. There are 2637 images of training images and 660 testing image. Figure 2 shows the sample images of ISIC-2019 dataset.



**Figure 2-**Sample input images

### 3.1.2. HAM10000

Figure 3 presents the sample image of this dataset.



**Figure 3**-Samples of HAM10000 dataset

Melanoma, nevus, basal cell carcinoma, vascular lesions, benign keratosis, and dermatofibroma are all shown in this group of photos (df). This collection contains 10,008 dermoscopic pictures. Bcc skin lesion subtypes comprise 514 of these photos. Ak skin lesion subtypes account for 327. Nv skin lesion subtypes comprise 6,705 of these photos..

### 3.2. Hair Removal

Erroneous segmentation can occur when recognising the border of skin lesions is hampered by the presence of hair and artefacts such air bubbles and light reflections. In order to remove hair from photos, the standard Dull Razor procedure is used as a pre-processing step. There are three key processes that make up the implementation of the DullRazor tool, which may be seen in the images shown in Figure 4:

- ❖ Closing procedure is used to identify the dark hair areas in general grayscale.
- ❖ A bilinear interpolation is used to replace the adjacent pixels that have been certified to be hair pixels.
- ❖ It uses an adaptive median filter to smooth the replacement hair pixels.

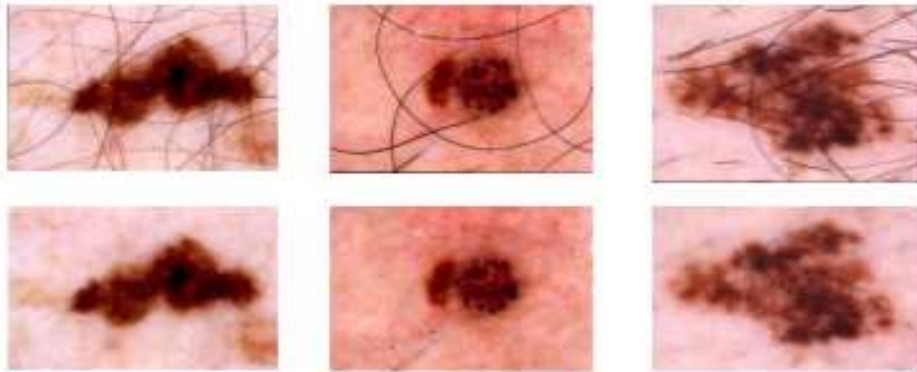


**Figure 4**-Example of Hair Removed Images

#### 3.2.1. Filtering hair removed images

Skin lesion photos can still show noise even after the hair has been removed. Scratches on the skin, like bubbles, produce noise. Filtering was used to eliminate them. The median filtering technique is employed in this investigation. An image's noise can be reduced in this way as a pre-processing step to enhance the outcomes of further processing.

### 3.3. Segmentation

Numerous studies have found that computer vision relies heavily on image segmentation [22]. It is common for segmentation algorithms to be applied to a certain class of photos. Images have been segmented using several ways in recent years. Segmentation is the process of dividing a suspicious lesion from the surrounding healthy skin in order to extract additional indications and features from the affected area. We can also streamline the classification

process with the use of automated segmentation. Mean shift segmentation is used in this study to identify the lesion's border from the surrounding skin.

**A. Segmenting Lesion Images**

We employed a semi-supervised mean-shift technique for segmentation based on the idea that pigmented skin lesions are depigmentation of the skin and to lessen computing costs. It is common practise to utilise the Mean-Shift technique to cluster a set of data points. The number of clusters does not have to be specified when using mean-shift instead of other parametric systems like k-means. The optimal number of clusters for the input data is determined by the algorithm itself. With the help of mean shift clustering, it is possible to build large, non-parametric clusters without having to know the number of clusters or even the shape of the clusters. As an empirical possibility, feature space is considered. As a rule of thumb, the mode (or local maxima) of a distribution's probability density function is a dense region (or cluster).

The underlying concept is straightforward, but the end effect is stunning. By specifying "Mean Shift," we mean When calculating the average value of the data points, it adjusts the window centre to the mean first, and then it repeats this process until convergence is reached. This method is called a "mean shift." Iteration after iteration, the window moves to a more concentrated area. The procedure that is used to perform mean-shift segmentation is as follows [22].

Mean-shift picture segmentation involves a series of processes.

- 1) Compute the RGB image's joint histogram.

Each colour is represented by a different number of clusters, a total of ten. As a result, a 1000-bin joint histogram will be generated. The spatial and colour ranges must be provided as inputs. The term "spatial range" refers to the range of pixels that should be taken into account while calculating the mean value for a given pixel. The colour gamut indicates which pixels in the surrounding area are most likely to be taken into account when rendering.



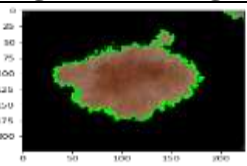


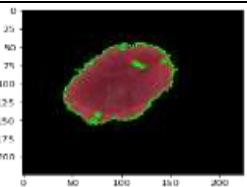
- 1) Compute the mean.

$$M = \text{sum}(m(i) * p(i)) / \text{sum}(p(i)) \tag{1}$$

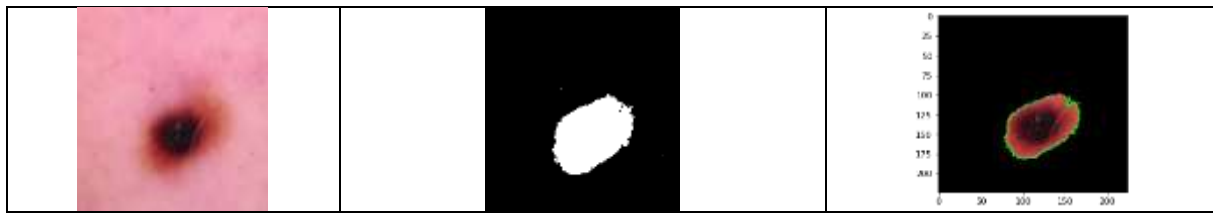
The pixel's mean value is represented by m(i), whereas the probability of the pixel falling into the m(i)th bin is represented by p(i). Up until a point of convergence, the mean is calculated with the neighbourhood and then with a new neighbourhood (iteratively). During each cycle, the distance between the pixel's source bin and its destination bin is measured.

- 2) Do this for each and every pixel in the picture. Table 1 displays the results of the skin pictures' segmentation, as seen in figure 5.

**Table.1-Segmentation Results**

Input	Black and white Image	Segmented image
		
		





### 3.4. Deep Forest

The segmented skin cancer images are given as an input for this classifier to predict the classification of skin cancer. The Deep Forest is an ensemble-based decision trees approach which emphasizes on building deep models using modules which are non-differentiable. It is built around 3 major principles which are considered to be the reasons behind the rich accomplishments of deep models. The reasons are as follows:

- ❖ Layer by Layer processing: It is considered one of the major factors since, no matter how complex the flat model becomes, the features of layer by layer processing cannot be achieved.
- ❖ In-model feature transformation: Basic machine learning models work on the original set of features. However, new features are generated during the learning process of a deep model.
- ❖ Appropriate model complexity: The fact that large datasets need complex models, basic machine learning models are limited in terms of complexity, however, it is not the case with deep models.

The overall structural working of the deep forest is separated under two broad parts Cascade Forest Structure & Multi-Grained Scanning. Cascade forest structure is employed to ensure the layer by layer processing while Multi-grained scanning allows the model to achieve sufficient complexity.

#### 3.4.1. Cascade Forest Structure

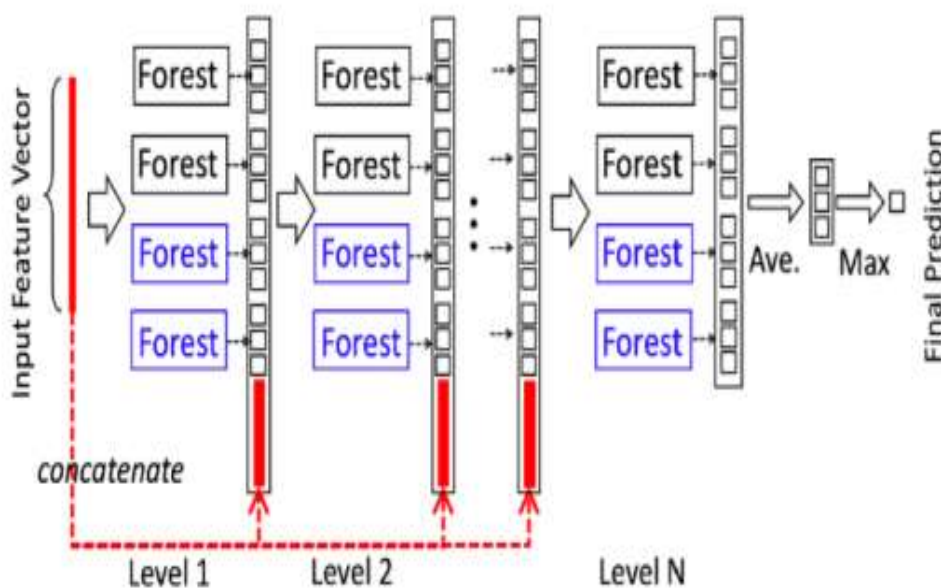


**Figure 5-Cascade forest construction**

A cascade structure is employed to represent the layer-by-layer processing of raw features. Each layer in the cascade takes input (processed information) from the previous layer and feeds it into the next layer. A layer in the structure can be defined as an ensemble of decision tree forests. It is ensured that diversity is maintained while creating ensembles by including different kinds of forests.

The working in cascading stage proceeds as follows, for a given case, an approximate of class distribution will be generated by each forest. This is done by taking into consideration the training examples and fraction of different classes at the terminal or leaf node where the

particular instance falls followed by averaging across all the trees in the same forest. This has also been depicted in Figure.5. The approximated class distribution so obtained forms a vector of classes with the help of k-fold cross-validation, the vector is then concatenated with the original set of features. The result is then forwarded to the next cascading layer. K-fold cross-validation helps in dropping the risk of overfitting. The number of levels is determined automatically based on the performance on the validation set.

A striking difference in the working of deep forest and other deep models is the ability to adaptively change the model complexity by terminating the amount of training data when tolerable. This provides a considerable advantage when working with datasets of varying sizes.

### 3.4.2. Multi-Grained Scanning

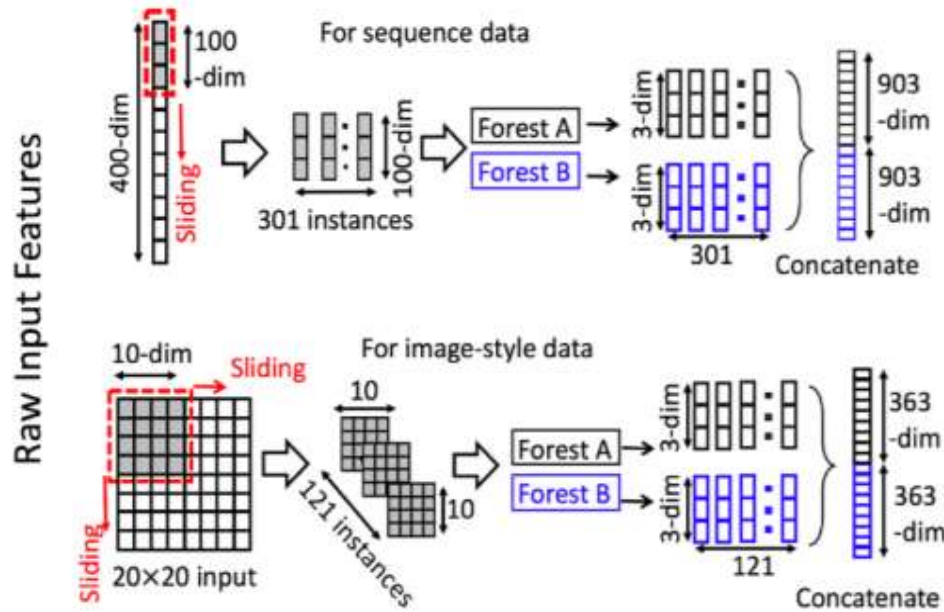


**Figure 6-**Multi-Grained scanning

The cascading forest procedure is enriched with the procedure of multi-grained scanning. The inspiration behind the inclusion of the multi grained scanning procedure was that deep models are generally well suited and also good at handling feature relationships. The whole procedure has been depicted in Figure 6. Raw features are scanned by the sliding windows and feature vectors are produced. The feature vectors are regarded as either negative or positive instances based on the extraction from the training sample; they are then used to produce class vectors. A completely random forest are trained using the instances extracted from windows having the same size. Transformed features are obtained by the concatenation of generated class vectors.

The actual label of the training sample is used to assign the instances that are extracted from the windows. Though these assignments can be incorrect, they can be attributed to the flipping output method. Also, feature sampling can be performed if transformed feature vectors are too long. The sliding windows size is varied to obtain grained features vectors that are different.

The Deep forest has shown a lot of promise and its success can be attributed to the following factors:

- ❖ Fewer hyper-parameters
- ❖ Data-dependent tuning of model's complexity
- ❖ Less dependence on GPU

The scalable manner uses distributed parallel ML algorithms with several optimisation strategies that enable it to manage very large network and host event volumes. The scalable design also enables a quick and parallel examination of network and host-level actions by using the overall graphic processing unit (GPU) processing capacity. Finally, this classifier can able to identify the skin cancer.

#### 4. Results and Discussion

We tested the segmentation and classification models on skin cancer segmentation and classification tasks in order to illustrate their performance. A single GPU system with 56GB of RAM and an NVIDIA GEFORCE GTX-1080 Ti GPU with 12GB of memory is utilised for this implementation of the TensorFlow DL framework.

##### 4.1. Evaluation metrics

Precision, recall, accuracy (AC), F1-score, Intersection over Union (IoU), and Dice Coefficient (DC) were all examined for quantitative analysis of the trial data (DI). To do this we also use the variables True Positive (TP), False Positive (FP), True Negative (TN) and False Negative (FN). The precision and recall are expressed as:

$$Precision = \frac{TP}{TP+FP} \quad (2)$$

$$Recall = \frac{TP}{TP+FN} \quad (3)$$

The accuracy is considered using Eq. (4),

$$AC = \frac{TP+TN}{TP+TN+FP+FN} \quad (4)$$

In addition, we tested Eq. to see if the IoU represented by it is accurate (5). The ground truth (GT) and segmentation result (SR) are used interchangeably here.

$$IoU = \frac{|GT \cap SR|}{|GT| + |SR|} \quad (5)$$

The F1-Score is calculated agreeing to the subsequent equation:

$$F1 - score = 2 \times \frac{precision \times recall}{precision + recall} \quad (6)$$

Furthermore, the Dice Coefficient (DI) is calculated using the following Eq. (7).

$$DI = \frac{2 \cdot TP}{2 \cdot TP + FN + FP} \quad (7)$$

##### 4.2. Performance Evaluation of Segmentation analysis

In this section, the comparative analysis is carried out between proposed mean-shift algorithm with existing techniques such as Otsu Algorithm [24] and Threshold algorithm [25] in terms of IoU and DI for two datasets, where these techniques are implemented in the work. Table 2 and Figure 7 shows the validated analysis of proposed segmentation technique.

**Table 2-**Comparative Analysis of Proposed Segmentation Technique in terms of DI and IoU

Method	Dataset	IoU	DI
Otsu Algorithm	ISIC 2019	0.6734	0.6845
Threshold		0.7645	0.7724
Proposed Mean-shift Algorithm		0.8821	0.8929
Otsu Algorithm	HAM10000	0.7167	0.7245
Threshold		0.7921	0.8097
Proposed Mean-shift Algorithm		0.8883	0.8960



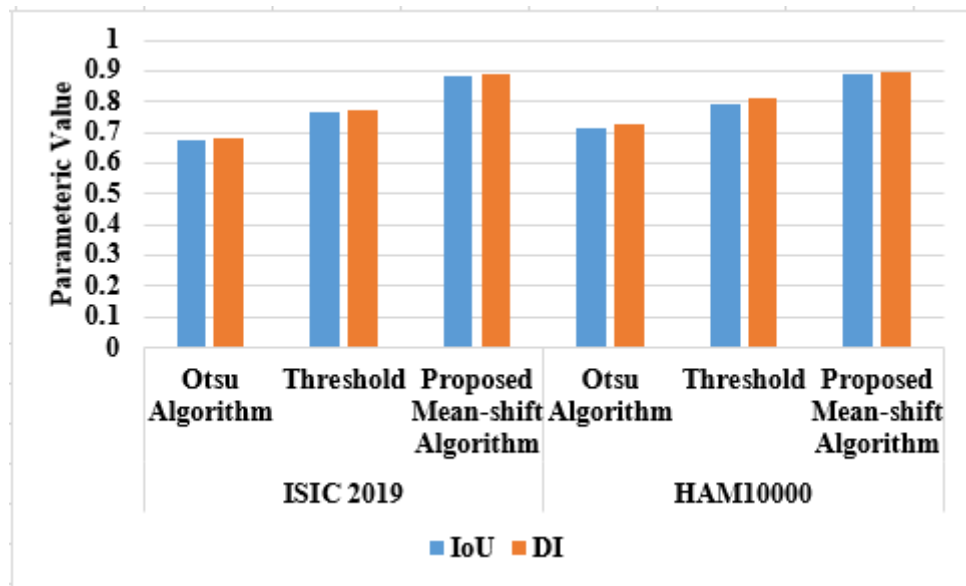


**Figure 7-**Graphical Representation of proposed segmentation model in terms of DI and IoU

In the ISIC 2019 dataset, the existing technique Otsu Algorithm achieved 0.6734IoU and 0.6845DI, Threshold algorithm achieved 0.7645IoU and 0.7724DI, where the proposed mean-shift algorithm achieved 0.8821IoU and 0.8929DI. In the analysis of HAM10000 dataset, the Otsu Algorithm achieved 0.7167IoU and 0.7245DI, Threshold algorithm achieved 0.7921IoU and 0.8097DI, where the proposed mean-shift algorithm achieved 0.8883IoU and 0.8960DI for the input images. The next section will describe the analysis of proposed classifier with existing techniques in terms of various parameters.

**4.3. Performance Analysis of Proposed Classifier**

In this section, the performance of proposed Deep Forest Classifier (DFC) is compared with existing Deep learning techniques such as Convolutional Neural Network (CNN) [26] and Generative Adversarial Network (GAN) [26] in terms of four parameters for two different datasets, where these techniques are implemented in this research work. Table 3 shows the experimental analysis of proposed classifier with existing techniques. Figure 8 shows the graphical representation of the DFC for ISIC 2019 dataset.

**Table 3-**Comparative Analysis of Proposed DFC for two datasets in terms of various parameter metrics

Method	Dataset	Precision	Recall	Accuracy	F1-measure
CNN	ISIC 2019	0.9166	0.8654	0.8697	0.8890
GAN		0.9167	0.9164	0.9034	0.9145
Proposed DFC		0.9668	0.9603	0.9603	0.9603
CNN	HAM10000	0.8077	0.8200	0.7866	0.8114
GAN		0.9266	0.9416	0.9226	0.9312
Proposed DFC		0.9707	0.9636	0.9636	0.9644

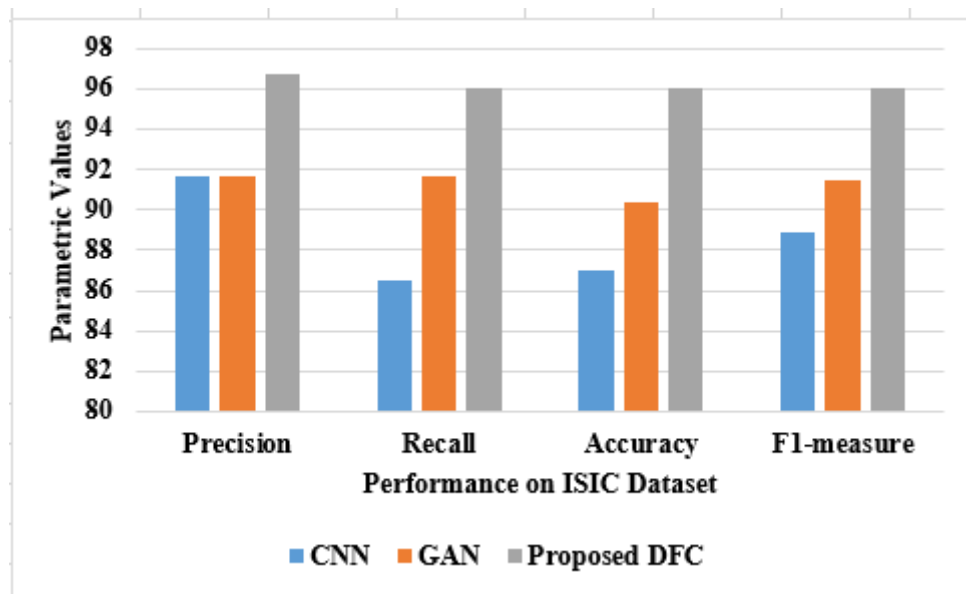


**Figure 8-**Graphical representation of proposed DFC with existing techniques for ISIC-2019 Dataset

In the precision analysis of ISIC-2019 dataset, the CNN achieved 91.66%, GAN achieved 91.67% and proposed DFC achieved 96.68%, where CNN, GAN and DFC achieved 86.54% of recall, 91.64% of recall and 96.03% of recall values on the same dataset. The accuracy and F-measure of DFC is 96.03%, where the CNN achieved nearly 87% and GAN achieved nearly 91% of accuracy and F-measure. DFC outperforms CNN and GAN because it doesn't take as much work in tweaking hyper-parameters, even when applied to a variety of datasets. Almost same hyper-parameter settings are required to get optimal performance. When learning to use DFC, users have the option of tailoring their training budget based on the amount of computational power they have at their disposal. For the HAM10000 dataset, the graphical depiction of the proposed DFC is shown in Figure 9.

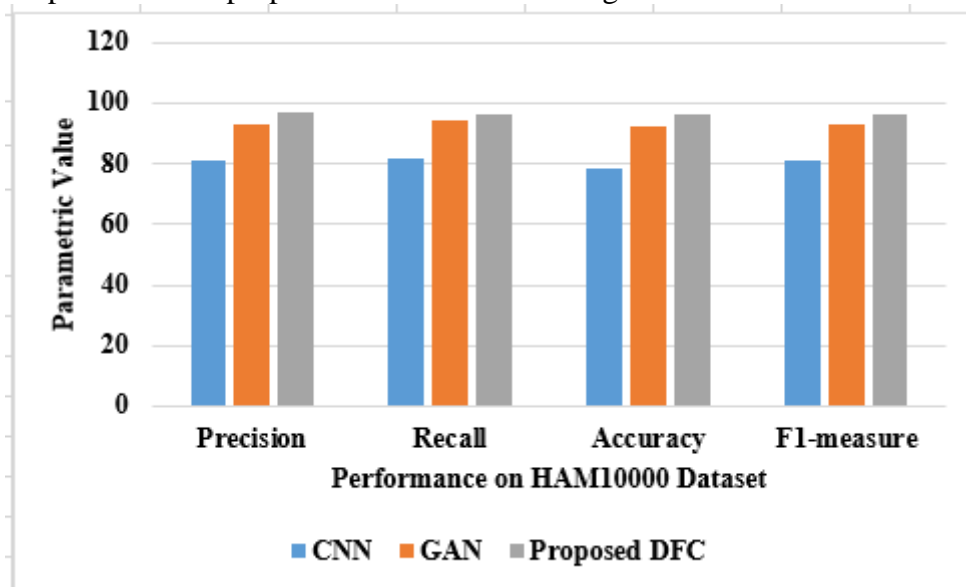


**Figure 9-**Graphical Representation of proposed DFC with existing techniques for HAM10000 Dataset

In the precision analysis of HAM10000 dataset, the CNN achieved 80.77%, GAN achieved 92.66% and proposed DFC achieved 97.07%, where CNN, GAN and DFC achieved

82.00% of recall, 94.16% of recall and 96.36% of recall values on the same dataset. The accuracy and F-measure of DFC is 96%, where the CNN achieved nearly 80% and GAN achieved nearly 92% of accuracy and F-measure. From these analysis, it is clearly shows that the proposed DFC achieved better performance than CNN and GAN. MobileNet [20] achieved 92.7% of accuracy and the same model from [21] achieved 83.1% of accuracy on HAM10000 dataset, where the proposed model achieved 96% of accuracy. The reason for better performance of DFC is that there are only two structures such as cascade and multi-grained scanning structures, where MobileNet has 53 layers deep, which is complex in structures.

## 5. Conclusion

Early control and mitigation of skin cancer can optimize a person's chance of survival. Due to the prevalence of distracting factors such as lighting fluctuation and light reflections off the skin surface, studying these dermoscopic images can indeed be difficult for dermatologists. The precise demarcation of the skin pathology area is critical in determining the type of skin illness. In this research work, semi-supervised mean shift algorithm is used for segmentation process and before segmentation, hair removal process is carried out by new tool called DullRazor. Finally, the segmented image is used as an input for proposed DFC to predict the skin cancer. The validation of proposed DFC is taken on two datasets such as ISIC-2019 and HAM10000 datasets and compared with existing techniques such as CNN and GAN. The results proved that DFC achieved 96% of accuracy on both datasets, where CNN achieved 86% on ISIC-2019 and 78% of accuracy on HAM10000 datasets. In future work, optimization of the deep network structures will also be explored to further evaluate efficiency of the resulting models.

## References

- [1] A. Naeem, M. S. Farooq, A. Khelifi, and A. Abid, "Malignant melanoma classification using deep learning: datasets, performance measurements, challenges and opportunities," *IEEE Access*, vol. 8, pp. 110575–110597, 2020.
- [2] H. Sung, J. Ferlay, R. L. Siegel et al., "Global cancer statistics 2020: GLOBOCAN estimates of incidence and mortality worldwide for 36 cancers in 185 countries," *CA: a cancer journal for clinicians*, vol. 71, no. 3, pp. 209–249, 2021.
- [3] C. Sinclair and P. Foley, "Skin cancer prevention in Australia," *British Journal of Dermatology*, vol. 161, pp. 116–123, 2009.
- [4] L. D. Marrett, P. De, P. Airia, and D. Dryer, "Cancer in Canada in 2008," *Canadian Medical Association Journal*, vol. 179, no. 11, pp. 1163–1170, 2008.
- [5] D. E. O'Sullivan, D. R. Brenner, P. A. Demers, J. V. Paul, M. F. Christine, and D. K. Will, "Indoor tanning and skin cancer in Canada: a meta-analysis and attributable burden estimation," *Cancer epidemiology*, vol. 59, pp. 1–7, 2019.
- [6] P. C. Marcelo de and P. Dubuisson, "An overview of the ultraviolet index and the skin cancer cases in Brazil," *Photochemistry and Photobiology*, vol. 78, 2003.
- [7] Z. Apalla, A. Lallas, E. Sotiriou, E Lazaridou, and D Ioannides, "Epidemiological trends in skin cancer," *Dermatology Practical & Conceptual*, vol. 7, pp. 1–6, 2017.
- [8] R. M. MacKie, "Clinical recognition of early invasive malignant melanoma," *BMJ* 301, 1005–1006 (1990).
- [9] N. R. Abbasi et al., "Early diagnosis of cutaneous melanoma: revisiting the ABCD criteria," *J. Am. Med. Assoc.* 292(22), 2771–2776 (2004).
- [10] R. B. Oliveira et al., "A computational approach for detecting pigmented skin lesions in macroscopic images," *Expert Syst. Appl.* 61, 53–63 (2016).
- [11] E. C. Murzaku, S. Hayan, and B. K. Rao, "Methods and rates of dermoscopy usage: a cross-sectional survey of US dermatologists stratified by years in practice," *J. Am. Acad. Dermatol.* 71, 393–395 (2014).
- [12] Dermatology Information System, <http://www.dermis.net/>.

- [13] N. C. F. Codella et al., "Skin lesion analysis toward melanoma detection: a challenge at the 2017 International Symposium on Biomedical Imaging (ISBI), hosted by the International Skin Imaging Collaboration (ISIC)," CoRR, arXiv:1710.05006 (2017).
- [14] N. C. Codella et al., "Skin lesion analysis toward melanoma detection: a challenge at the 2017 International Symposium on Biomedical Imaging (ISBI)," hosted by the International Skin Imaging Collaboration (ISIC), in IEEE 15th Int. Symp. Biomed. Imaging (ISBI), IEEE, pp. 168–172 (2018).
- [15] Hameed, N., Shabut, A.M. and Hossain, M.A., "Multi-Class Skin Diseases Classification Using Deep Convolutional Neural Network and Support Vector Machine," 12th International Conference on Software, Knowledge, Information Management & Applications (SKIMA), Phnom Penh, 3-5 December 2018, Vol. 1, 14-20.
- [16] Ahmed, Md.H., Ema, R.R. and Islam, T., "An Automated Dermatological Images Segmentation Based on a New Hybrid Intelligent ACO-GA Algorithm and Diseases Identification Using TSVM Classifier," 1st International Conference on Advances in Science, Engineering and Robotics Technology, Dhaka, 3-5 May 2019, 894-899.
- [17] Khan, M.Q., Hussain, A., Ur Rehman, S., Khan, U., Maqsood, M., Mehmood, K. and Khan, M.A., "Classification of Melanoma and Nevus in Digital Images for Diagnosis of Skin Cancer," IEEE Access, 7, 90132-90144, 2019.
- [18] Hameed, N., Shabut, A.M. and Hossain, M.A., "A Computer-Aided Diagnosis System for Classifying Prominent Skin Lesions Using Machine Learning," 10th Computer Science and Electronic Engineering (CEEC), Colchester, 19-21 September 2018, Vol. 1, 86-91.
- [19] T. J. Brinker et al., "A convolutional neural network trained with dermoscopic images performed on par with 145 dermatologists in a clinical melanoma image classification task," Eur. J. Cancer, 2019, doi: 10.1016/j.ejca.2019.02.005.
- [20] E. H. Mohamed and W. H. El-Behaidy, "Enhanced Skin Lesions Classification Using Deep Convolutional Networks," Proc. - 2019 IEEE 9th Int. Conf. Intell. Comput. Inf. Syst. ICICIS 2019, pp. 180188, 2019, doi: 10.1109/ICICIS46948.2019.9014823.
- [21] S. S. Chaturvedi, K. Gupta, and P. S. Prasad, "Skin lesion analyser: an efficient seven-way multi-class skin cancer classification using mobilenet," Adv. Intell. Syst. Comput., vol. 1141, pp. 165176, 2019, doi: 10.1007/978-981-15-3383-9\_15.
- [22] Sreelatha, T., Subramanyam, M.V. and Prasad, M.N., "Early detection of skin cancer using melanoma segmentation technique. Journal of medical systems, 43(7), pp.1-7, 2019.
- [23] Sumithra, R.; Suhil, M.; Guru, D.S., "Segmentation and Classification of Skin Lesions for Disease Diagnosis," Proc. Comput. Sci. 2015, 45, 76–85.
- [24] Zhang J, Hu J., "Image segmentation based on 2d otsu method with histogram analysis," In: 2008 International conference on computer science and software engineering, vol 6. IEEE, pp 105–108, (2008).
- [25] M. E. Celebi, S. Hwang, H. Iyatomi, and G. Schaefer, "Robust border detection in dermoscopy images using threshold fusion," In 2010 IEEE International Conference on Image Processing, pages 2541-2544, September 2010.
- [26] Sedigh, P., Sadeghian, R. and Masouleh, M.T., "Generating synthetic medical images by using GAN to improve CNN performance in skin cancer classification. In 2019 7th International Conference on Robotics and Mechatronics (ICRoM) (pp. 497-502). IEEE, November - 2019.